Dig Dis Sci (2016) 61:1107–1120
DOI 10.1007/s10620-015-3976-2

ORIGINAL ARTICLE

Regulatory Effects and Mechanism of Adenovirus-Mediated PTEN Gene on Hepatic Stellate Cells

Junyan An[1] · Libo Zheng[1] · Shurui Xie[1] · Fengrong Yin[1] · Xiaoxia Huo[1] · Jian Guo[1] · Xiaolan Zhang[1]

Received: 6 November 2014 / Accepted: 23 November 2015 / Published online: 12 December 2015

Abstract

Background Tension homology deleted on chromosome ten (PTEN) is important in liver fibrosis.

Aims The purpose of this study was to evaluate the PTEN gene effects and mechanism of action on hepatic stellate cells (HSCs).

Methods The rat primary HSCs and human LX-2 cells were transfected by an adenovirus containing cDNA constructs encoding the wild-type PTEN (Ad-PTEN), the PTEN mutant G129E gene (Ad-G129E) and RNA interference targeting the PTEN sequence PTEN short hairpin RNA (PTEN shRNA), to up-regulate and down-regulate PTEN expression, respectively. The HSCs were assayed with a fluorescent microscope, real time PCR, Western blot, MTT, flow cytometry and Terminal-deoxynucleoitidyl transferase mediated nick end labeling. In addition, the CCl_4 induced rat hepatic fibrosis model was also established to check the in vivo effects of the recombinant adenovirus with various levels of PTEN expression.

Results The data have shown that the over-expressed PTEN gene led to reduced HSCs activation and viability, caspase-3 activity and cell cycle arrest in the G_0/G_1 and G_2/M phases, as well as negative regulation of the PI3K/Akt and FAK/ERK signaling pathways in vitro. The over-expressed PTEN gene improved liver function, inhibited proliferation and promoted apoptosis of HSCs both in vitro and in vivo.

Conclusions These data have shown that gene therapy using the recombinant adenovirus encoding wild-type PTEN inhibits proliferation and induces apoptosis of HSCs, which is a potential treatment option for hepatic fibrosis.

Keywords PTEN · Hepatic stellate cell · Hepatic fibrosis · Gene therapy

Abbreviations

HSCs	Hepatic stellate cells
ECM	Extracellular matrix
α-SMA	Alpha-smooth muscle actin
PTEN	Tension homology deleted on chromosome ten
BDL	Bile duct ligation
shRNA	Short hairpin RNA
GFP	Green fluorescent protein
EGFP	Enhanced green fluorescent protein
H&E	Hematoxylin and eosin
MT	Masson's trichrome
TUNEL	Terminal-deoxynucleoitidyl transferase mediated nick end labeling
FCM	Flow cytometry
FAK	Focal adhesion kinase
ERK	Extracellular signal-regulated kinase
PI3K	Phosphoinositol-3-kinase
Akt	Serine–threonine protein kinase B
ALT	Alanine aminotransferase
AST	Aspartate aminotransferase

Junyan An and Libo Zheng have contributed equally to this work.

✉ Xiaolan Zhang
xiaolanzh@126.com

[1] Department of Gastroenterology, The Second Hospital of Hebei Medical University, Hebei Key Laboratory of Gastroenterology, Hebei Institute of Gastroenterology, 215 West Heping Road, Shijiazhuang 050000, Hebei, China

Introduction

Hepatic fibrosis results from chronic liver injury and is considered to be reversible; however, the resulting end stage cirrhosis is irreversible and can cause additional complications, as well as high mortality [1, 2]. Hepatic stellate cells (HSCs) activate and proliferate under fibrogenic conditions and are believed to be the major source of resident myofibroblasts in the fibrotic liver [3–5]. With the appearance of characteristic activation marker alpha-smooth muscle actin (α-SMA), the HSCs become active and increase the synthesis and deposition of ECM components in the liver [6]. Therefore, HSCs are an attractive target for anti-fibrotic therapy [7, 8].

Phosphatase and tension homolog deleted on chromosome ten (PTEN), the first tumor-suppressing gene found to have dual protein/lipid phosphatase activity, negatively regulates the cell cycle, decreases cell proliferation and promotes apoptosis of tumor cells [9–12]. Earlier PTEN studies have focused on non-tumor diseases and have shown that PTEN inhibits proliferation and induces apoptosis of lung fibroblasts in vitro [13, 14], while the lower expression of PTEN can also cause renal fibrosis [15]. The absence of PTEN in specific hepatic cells may result not only in hepatocellular carcinoma, but also in nonalcoholic steatohepatitis, which has been found to be closely associated with hepatic fibrosis [16].

Our previous study has shown that PTEN expression decreased in fibrotic rat hepatic tissues induced by bile duct ligation (BDL) [17]. During the reversal of liver fibrosis pretreated by CCl_4, the PTEN mRNA and protein expression returned to almost normal levels, showing a connection between PTEN and the stage of rat hepatic fibrosis [18]. However, the mechanism of PTEN gene effects on proliferation and apoptosis of primary HSCs remains unclear.

This study was designed to investigate the effects of over-expressed PTEN on proliferation, apoptosis and cell cycle of HSCs in vitro and in vivo, which may provide a new strategy for prevention and treatment of liver fibrosis.

Materials and Methods

Animals

Adult male Wistar rats, 8 weeks old and weighing 350–400 g, were obtained from the Experimental Animal Center of the Hebei Medical University. The whole experiment was performed in compliance with the national ethical guidelines for the care and use of laboratory animals, following internationally accepted principles of laboratory animal use and care defined in US guidelines (NIH publication #85-23, revised in 1985).

Rat Primary HSCs Isolation and Cell Culture

Rat primary HSCs were isolated from normal healthy male Wistar rats using in situ recirculating perfusion technology, as described [19]. The cells were then cultured in DMEM with 10 % FBS. The first medium change was performed at 24 h post-isolation. The cells were passaged at days 15 and 25 post-isolation and the second passage was used for transfection. The purification degree of primary HSCs at passage 2 was higher than 95 %.

Human LX-2 cells were obtained from the Mount Sinai School of Medicine.

Recombinant Adenovirus and Transfection

The adenovirus containing cDNA constructs encoding wild-type PTEN (Ad-PTEN) with a green fluorescent protein (GFP), the PTEN mutant G129E gene (Ad-G129E) with GFP and the empty virus control (Ad-GFP) were provided by Prof. Junshan Zhu from the Third Military Medical University in China. The RNA interference targeting PTEN sequence, and the PTEN short hairpin RNA (shRNA) with enhanced green fluorescent protein (EGFP) was established by Wuhan Genesil Biotechnology Co., Ltd (Wuhan, China). The transfection was performed as described [20] and confirmed by demonstrating GFP expression in rat primary HSCs. The infection efficiency of the adenovirus was determined using fluorescence microscopy and flow cytometry (data not shown). For optimal transfection, we used the MOI 50 for 72 h (rat primary HSCs infection efficiency: 94.46 %; human LX-2 cells infection efficiency: 89.89 %).

The rat primary HSCs and human LX-2 cells were divided into five groups: (1) the control group, antibiotics-free DMEM; (2) the Ad-GFP group, with Ad-GFP transfection; (3) the Ad-PTEN group, with Ad-PTEN transfection; (4) the Ad-G129E group, with Ad-G129E transfection; and (5) the PTEN shRNA group, with PTEN shRNA transfection.

Real Time PCR

Real time PCR was performed as previously described [18, 21]. Primer Express 5.0 was used to design the following primers: PTEN (rat) Forward 5′-GGA AAG GAC GGA CTG GTG TA-3′, Reverse 5′-GGA AAG GAC GGA CTG GTG TA-3′; PTEN (human) Forward 5′-ACC GCC AAA TTT AAT TGC AG-3′, Reverse 5′-GGG TCC TGA ATT GGA GGA AT-3′; PI3K (rat) Forward 5′-ACT TTG TGA CCT TCG GCT TT-3′, Reverse 5′-TAC ATT CCT GAT

CTT CCT CG-3′; PI3K (human) Forward 5′-TGC CTC CAC GAC CAT CAT CA-3′, Reverse 5′-TTC ACA CAC TGG CAT GCC GA-3′; Akt (rat) Forward 5′-GAG GAG CGG GAA GAG TG-3′, Reverse 5′-GAG ACA GGT GGA AGA AGA GC-3′; Akt (human) Forward 5′-CAT CAC ACC ACC TGA CCA AG-3′, Reverse 5′-CTC AAA TGC ACC CGA GAA AT-3′; FAK (rat) Forward 5′-ACT TGG ACG CTG TAT TGG AG-3′, Reverse 5′-CTG TTG CCT GTC TTC TGG AT-3′; FAK (human) Forward 5′-GCG TCT AAT CCG ACA GCA-3′, Reverse 5′-GCC GAC TTC CTT CAC CAT-3′; ERK1 (rat) Forward 5′-TCA TAG GCA TCC GAG ACA TC-3′, Reverse 5′-TGG TAG AGG AAG TAG CAG ATG-3′; ERK1 (human) Forward 5′-GAT GGG GCA GTA CAA GGA GA-3′, Reverse 5′-TGC AGT GGA TAG AGC ACC AG-3′; Rat collagen α1 (I) Forward: 5′-CAG GCT GGT GTG ATG GGA TT-3′, Reverse 5′-CCA AGG TCT CCA GGA ACA CC-3′; GAPDH (rat) Forward 5′-GGC AAG TTC AAC GGC ACA G-3′, Reverse 5′-CGC CAG TAG ACT CCA CGA CAT-3′; GAPDH (human) Forward 5′-ACT TTG GTA TCG TGG AAG GAC T-3′, Reverse 5′-GTA GAG GCA GGG ATG ATG TTC T-3′. The primers were synthesized by SBS Genetech Co., Ltd (Beijing, China). Relative mRNA expression was measured according to the method of fold increase ($2^{-\triangle\triangle Ct}$).

Western Blot Assay

Total protein was isolated either from the HSCs at 72 h post-infection or from the liver tissue of sacrificed rats. Western blotting was performed as previously described [17]. The anti-PTEN (Santa Cruz, USA), anti-Bcl-2 (Santa Cruz, USA), anti-Bax (Santa Cruz, USA), anti-CyclinD1 (Santa Cruz, USA), anti-CDK4 (Santa Cruz, USA), anti-$P27^{kip1}$ (eBioscience, USA), anti-Akt (eBioscience, USA), anti-p-Akt^{Thr308} (eBioscience, USA), anti-FAK (Santa Cruz, USA), anti-$pFAK^{Tyr397}$ (Santa Cruz, USA), anti-ERK1 (Santa Cruz, USA), anti-pERK1 (Santa Cruz, USA) (1:200) and anti-GAPDH antibodies (Santa Cruz, USA) (1:500) were used as primary antibodies. The blots were developed using enhanced chemiluminescene (ECL).

The results were analyzed with Kodak 1D digital imaging software (Kodak, USA) and reported as the optical density ratio of the target protein to GAPDH.

Cell Proliferation Assay with MTT

The MTT assay was performed as described previously [21]. Briefly, the HSCs were seeded into a 96-well plate at a density of 3×10^4/mL × 200 μL/well. Adenoviral gene transfection was performed as described above. At 24, 48 and 72 h post-infection, the MTT solution of 5 mg/mL × 20 μL/well was added to the wells. The cells were allowed to grow for 4 h and then the medium was replaced with 150 μL dimethylsulfoxide (DMSO). The absorbance (A), measured at 490 nm, was used to calculate the inhibition rate of proliferation [$(A_{control} - A_{experimental})/A_{control} \times 100$ %].

Apoptosis Assay by FAC and TUNEL

The cultured HSCs were analyzed by FAC and terminal-deoxynucleoitidyl transferase mediated nick end labeling (TUNEL) analysis to assay apoptosis, as previously described [21]. The double immunofluorescent staining of TUNEL and α-SMA was also done to study the apoptotic index of activated HSCs in vitro and in vivo [18].

Caspase-3 Activity Assay

We used the caspase activity assay kit from Beyotime Institute of Biotechnology (China) to measure caspase-3 activity, according to manufacturer's instructions. Briefly, 5×10^4 HSCs/mL were seeded into each well in a 6-well plate and infected by the corresponding virus. The cells were harvested and lysed for 15 min on ice in a ratio of 200,000 cells to 100 μL of the lysis buffer. Protein concentration was measured using the Bradford assay kit to determine the suitable amount of protein for the next step. In a 96-well plate, 80 μL of detection buffer + 10 μL sample + 10 μL Ac-DEVD-pNA was added into each well at 37 °C for 4 h. Then A405 was measured to determine caspase-3 activity.

Cell Cycle Assay by FAC

A total of 5×10^4 HSCs/mL were seeded into each well in a 6-well plate and infected by the virus. The cells were harvested and adjusted to 1×10^6/mL using 1 × PBS. Then, 100 μL of this cell solution were added to 1 mL of the PI buffer in the dark, at 4 °C, for 30 min. The cell solution was filtered before acquiring the data. Chicken erythrocytes also underwent the same process. The data was analyzed using Expo 32 ADC and Muticycle AV.

Animal Model

CCl_4-induced rat hepatic fibrosis was established as described previously [18]. Recombinant adenovirus (2×10^9 pfu/100 μL/rat) was introduced by injecting the tail vein of the rats once per week, starting at the fourth week post-administration of CCl_4 and lasting for 4 weeks. Recombinant adenoviruses used in the in vivo experiment were Ad-GFP, Ad-PTEN, Ad-G129E and PTEN shRNA; the CCl_4 only-treated rats were used as the control.

Pathology, Immunohistochemical and Immunofluorescent Staining of the Liver Tissue

Postmortem, the liver was removed and liver sections were processed routinely. Hematoxylin-eosin (H&E) staining was performed to assess the degree of inflammation and Masson's trichrome (MT) staining was performed to assess collagen deposition. Histopathological scores of the liver were assigned in a blinding manner by two well-trained pathologists—inflammation was graded according to the histology activity index (HAI-Knodell score) as Knodell [22]; fibrosis in the liver was analyzed by the Masson-stained area as percentage of the total area using ImageJ 2, as previously described [23]. To check the expression changes of PTEN in the liver tissue and HSCs in vivo, immunofluorescent staining was also performed on frozen liver sections, as described [18].

Statistical Analysis

The data were presented as the mean ± SD and analyzed with SPSS 18.0 software. One-way ANOVA, the Student–Newman–Keulsthe (SNK-q) test and the Student's t test were performed. $P < 0.05$ was considered to indicate a statistically significant difference.

Results

Effect of the PTEN Gene Expression on Proliferation of HSCs

The MTT results have shown that the wild-type PTEN and G129E genes were able to significantly inhibit the proliferation and viability of both rat primary HSCs (74.71 %) and human LX-2 cells (50.43 %) (Fig. 1a), while PTEN shRNA significantly enhanced the viability (118.26 vs 142.15 %) in comparison to the control group, $P < 0.01$ (Fig. 1a).

The BrdU assay was also used to check HSCs proliferation. At 72 h post-transfection, the DNA synthesis of primary HSCs and human LX-2 cells was significantly reduced in Ad-PTEN (63.32 vs 42.38 %) and Ad-G129E (74.75 vs 56.65 %) groups, compared to the Ad-GFP group ($P < 0.01$); whereas PTEN shRNA enhanced the DNA synthesis of rat primary HSCs by 35.36 %, $P < 0.01$, and human LX-2 cells by 57.13 %, $P < 0.01$ (Table 1).

Effect of PTEN Gene Expression on Apoptosis of HSCs

To further assess the regulation of the PTEN gene on HSCs, flow cytometry was performed using combined marked Annexin-V/PE to check the apoptosis of rat primary HSCs and human LX-2 cells. At 72 h post-transfection, significantly higher apoptotic rates of rat primary HSCs and human LX-2 cells were found in the Ad-PTEN (34.85 ± 2.11 vs 41.76 ± 1.98 %) and Ad-G129E (25.18 ± 1.34 vs 37.18 ± 2.13 %) groups in comparison to the control (3.12 ± 0.15 vs 5.68 ± 1.15 %) and Ad-GFP (4.21 ± 0.35 vs 7.21 ± 1.25 %) groups, with $P < 0.01$. In addition, significantly lower apoptotic rates were found in the PTEN shRNA group (1.24 ± 0.08 vs 2.25 ± 1.18 %) in comparison to the control and Ad-GFP groups, $P < 0.01$ (Fig. 1b). Additionally, TUNEL was also performed to double check the apoptosis of HSCs; similar results were found as in the case of Annexin-V staining assessed by flow cytometry (Fig. 1c).

To further investigate the mechanism of PTEN-induced HSCs apoptosis, we used Western blotting to check the expression of apoptosis-associated proteins and found that the expression of the Bcl-2 protein was decreased significantly in comparison to the control and Ad-GFP groups ($P < 0.01$). On the contrary, Bax protein expression significantly increased compared to the control and Ad-GFP groups ($P < 0.01$) by over-expression of the wild-type PTEN gene or G129E gene in rat primary HSCs and human LX-2 cells, with an enhanced ratio of Bax/Bcl-2 as well. Down-regulated PTEN expression in the PTEN shRNA group showed a completely opposite effect on Bcl-2 and Bax (Fig. 1d, e).

Fig. 1 Proliferation and apoptosis of HSCs detected at 72 h post-infection. **a** The MTT was used to detect the cell viabilities of rat primary HSCs and human LX-2 cells. At 72 h post-transfection, the viabilities of rat primary HSCs and human LX-2 cells were significantly reduced to 74.71 and 50.43 %, respectively, in comparison to the control group (100 %), $P < 0.01$, while PTEN shRNA significantly enhanced the viability to 118.26 and 142.15 % compared to the control group (100 %), $P < 0.01$. **b** Annexin-V/PE staining via FAC was used to check the apoptotic rate of HSCs, and find that the apoptotic rates of rat primary HSCs and human LX-2 cells in the Ad-PTEN group (34.85 ± 2.11 vs 41.76 ± 1.98 %) and the Ad-G129E group (25.18 ± 1.34 vs 37.18 ± 2.13 %) were significantly higher than the control group (3.12 ± 0.15 vs 5.68 ± 1.15 %) and the Ad-GFP group (4.21 ± 0.35 vs 7.21 ± 1.25 %), $P < 0.01$; while significantly lower apoptotic rates were found in the PTEN shRNA group (1.24 ± 0.08 vs 2.25 ± 1.18 %) as compared to the control group and Ad-GFP, $P < 0.01$. **c** TUNEL was also used to observe the apoptosis of HSCs, and results were observed under light microscope where the nuclei of apoptotic HSCs yielded a brown-colored positive reaction to show similar results as Annexin-V staining by flow cytometry. **d**, **e** Western blot was used to check the apoptosis-related protein expression for bcl-2 and bax. Bcl-2 protein expression significantly decreased in the Ad-PTEN and Ad-G129E groups while bax significantly increased compared to the control and Ad-GFP groups, $P < 0.01$, leading to an enhanced ratio of Bax/Bcl-2. The PTEN shRNA showed a completely opposite effect on Bcl-2 and Bax. $^{*}P < 0.01$, compared to the control group. $^{\#}P < 0.01$, compared to the Ad-GFP group $^{\S}P < 0.05$, compared to the Ad-PTEN group

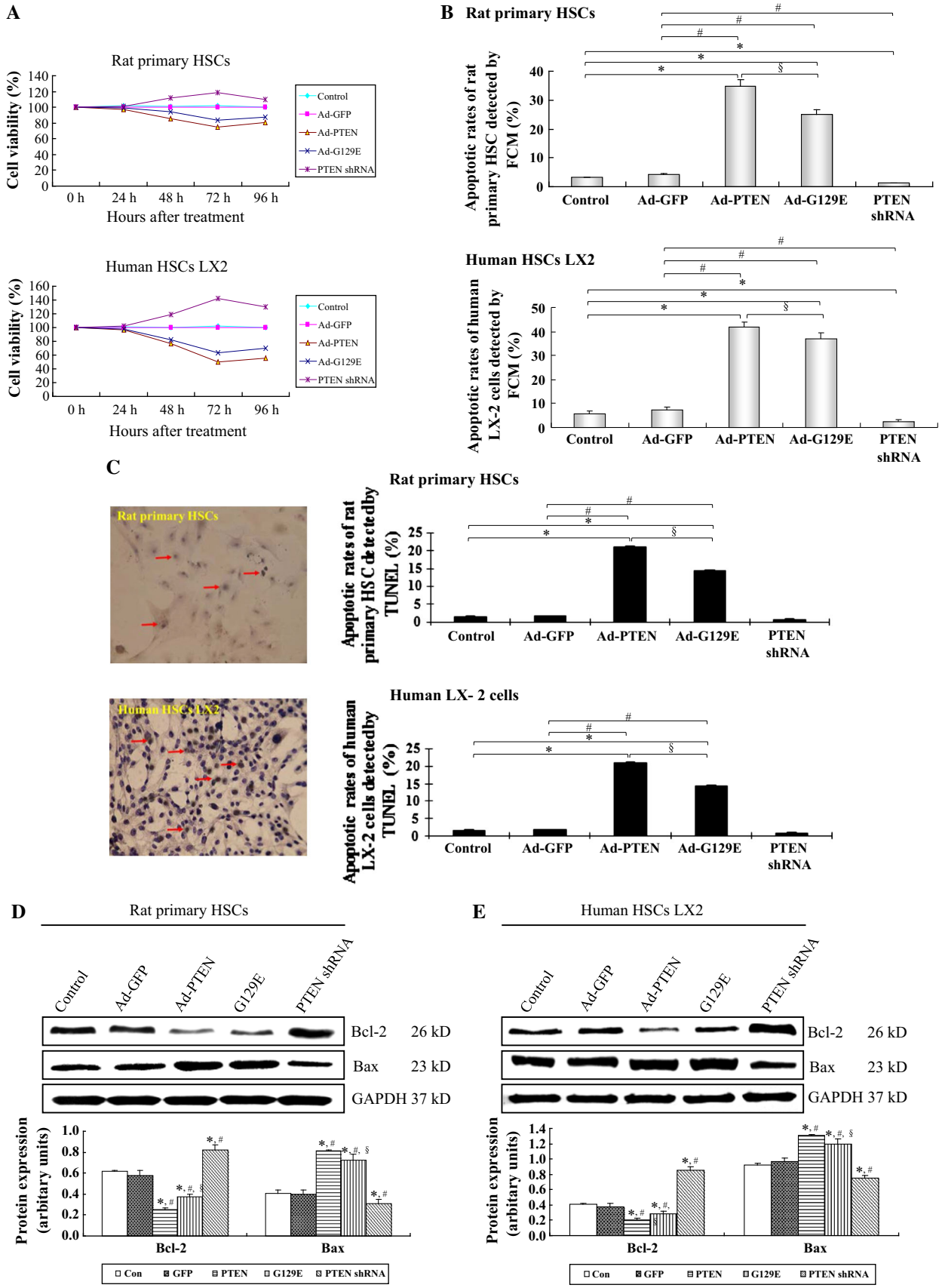
A
Rat primary HSCs
Cell viability (%)
Hours after treatment
0 h
24 h
48 h
72 h
96 h
Control
Ad-GFP
Ad-PTEN
Ad-G129E
PTEN shRNA
Human HSCs LX2
B
Rat primary HSCs
Apoptotic rates of rat primary HSC detected by FCM (%)
Human HSCs LX2
Apoptotic rates of human LX-2 cells detected by FCM (%)
C
Rat primary HSCs
Human HSCs LX2
Apoptotic rates of rat primary HSC detected by TUNEL (%)
Human LX- 2 cells
Apoptotic rates of human LX-2 cells detected by TUNEL (%)
D
Rat primary HSCs
Control
Ad-GFP
Ad-PTEN
G129E
PTEN shRNA
Bcl-2 26 kD
Bax 23 kD
GAPDH 37 kD
Protein expression (arbitary units)
Con
GFP
PTEN
G129E
PTEN shRNA
E
Human HSCs LX2

Table 1 The effects of PTEN on DNA synthesis of primary rat HSCs and LX-2 cells by BrdU assay (mean ± SD, $n = 6$)

Groups	DNA synthesis (%)	
	Rat primary HSCs	LX-2
Control	101.65 ± 1.34	100.34 ± 2.35
Ad-GFP	100.00 ± 0.00	100.00 ± 0.00
Ad-PTEN	63.32 ± 2.58[a]	42.38 ± 1.05[a]
Ad-G129E	74.75 ± 1.56[a]	56.65 ± 2.19[a]
PTEN shRNA	135.36 ± 4.65[a]	157.13 ± 5.32[a]

The DNA synthesis of rat primary HSCs and human LX-2 cells was significantly reduced in Ad-PTEN and Ad-G129E groups compared to the Ad-GFP group, whereas PTEN shRNA enhanced the DNA synthesis of rat primary HSCs and human LX-2 cells

[a] $P < 0.01$, in comparison to the control and Ad-GFP groups

Effect of PTEN Gene Expression on Caspase-3 Activity in HSCs

Over-expression of the wild-type PTEN gene and G129E gene significantly promoted the activity of caspase-3 in rat primary HSCs (2.16- vs 1.73-fold), $P < 0.01$, while, on the contrary, PTEN shRNA inhibited the activity of caspase-3 compared to the Ad-GFP group ($P < 0.05$). Similar results were also found in human LX-2 cells (Table 2).

Modulation of Cell Cycle by PTEN Gene Expression

Flow cytometry was used to check the cell cycles of rat primary HSCs and human LX-2 cells. A significantly greater number of cells was found in the G_0/G_1 phase in the Ad-PTEN (70.56 ± 4.05 vs 71.84 ± 2.15 %) and Ad-G129E (67.42 ± 2.15 vs 64.12 ± 1.25 %) groups, in comparison to the Ad-GFP group (58.78 ± 1.11 vs 56.37 ± 1.12 %), $P < 0.01$; while a significantly lower number of cells was found in the PTEN shRNA group (35.46 ± 3.05 vs 37.98 ± 2.13 %), $P < 0.01$. In the S phase, in comparison to the Ad-GFP group, significantly lower numbers of rat primary HSCs and human LX-2 cells were found in the Ad-PTEN (10.25 ± 1.04 vs 10.56 ± 1.15 %) and Ad-G129E (12.11 ± 1.05 vs 13.12 ± 3.12 %) groups in comparison to the Ad-GFP group (15.55 ± 1.74 vs 16.21 ± 2.13 %), $P < 0.01$; while a significantly lower number of cells was observed in the PTEN shRNA group (21.17 ± 2.94 vs 33.34 ± 2.15 %), $P < 0.01$. Cells in the G_2/M phase were also studied and found to be similar as cells in the S phase (Fig. 2a). These data indicated that both rat primary HSCs and human LX-2 cells were arrested in the G_0/G_1 and G_2/M phase by wild-type PTEN gene and G129E gene, while the PTEN shRNA acted as a promoter in this phase of the cell cycle.

Table 2 Over-expression of wild type PTEN gene increases caspase-3 activity in rat primary HSCs and human LX2 cells (mean ± SD, $n = 3$)

Groups	Caspase-3 activity (unit)	
	Primary rat HSCs	LX2
Control	3.45 ± 1.14	2.75 ± 1.23
Ad-GFP	3.37 ± 1.29	2.82 ± 1.02
Ad-PTEN	7.27 ± 2.18[a]	7.13 ± 2.37[a]
Ad-G129E	5.83 ± 1.25[a]	5.53 ± 1.37[a]
PTEN shRNA	1.28 ± 0.67[b]	0.81 ± 0.42[b]

Over-expression of wild-type PTEN and G129E genes significantly promoted the activity of caspase-3 while PTEN shRNA inhibited the activity of caspase-3 compared to the Ad-GFP group in both rat primary HSCs and human LX-2 cells

[a] $P < 0.01$, compared to the control and Ad-GFP groups

[b] $P < 0.05$, compared to control, Ad-GFP, and Ad-PTEN groups

To further investigate the mechanism of PTEN gene modulation on HSCs cell cycles, we detected several cell cycle-related protein expressions in rat primary HSCs and human LX-2 cells. We found significantly down-regulated CyclinD1 (29.07 vs 15.12, 38.79 vs 19.31 %) and CDK4 (42.96 vs 34.51, 33.67 vs 27.55 %) expression in the Ad-PTEN and Ad-G129E groups and significantly up-regulated $P27^{kip1}$ expression (63.16 vs 38.10, 67.37 vs 45.26 %) compared to Ad-GFP group ($P < 0.01$), while the PTEN shRNA had an opposite effect (Fig. 2b, c).

Signaling Transduction Mechanisms of PTEN in Behavior Regulation of HSCs

Western blotting has shown that, in rat primary HSCs, both PI3K and p-Akt^{Thr308} protein expression significantly decreased in the Ad-PTEN group (0.49 ± 0.02 vs 0.28 ± 0.02), in comparison with the Ad-G129E (0.75 ± 0.06 vs 0.48 ± 0.03), control (0.82 ± 0.07 vs 0.50 ± 0.02) and Ad-GFP (0.79 ± 0.03 vs 0.52 ± 0.05) groups ($P < 0.01$), while both of them showed opposite expressions in the PTEN shRNA group (1.12 ± 0.14 vs 0.62 ± 0.03) (Fig. 3a, b). A similar tendency was also found in experiments with human LX-2 cells (Fig. 3a, c). Real-time PCR was also used to check the changes in mRNA in primary HSCs. Expression of the control group was arbitrarily assigned a value of 1; then the PI3K mRNA relative expression levels in Ad-GFP, Ad-PTEN, Ad-G129E and PTEN shRNA groups were calculated to be 0.979-, 0.716-, 0.962- and 1.223-fold, respectively (Fig. 3d). Similar results were found in human LX-2 cells (Fig. 3e); however, no significant differences were found in the Akt mRNA expressions (Fig. 3d, e). The data indicated that PTEN may regulate HSCs behavior via the PI3K/Akt signaling pathway.

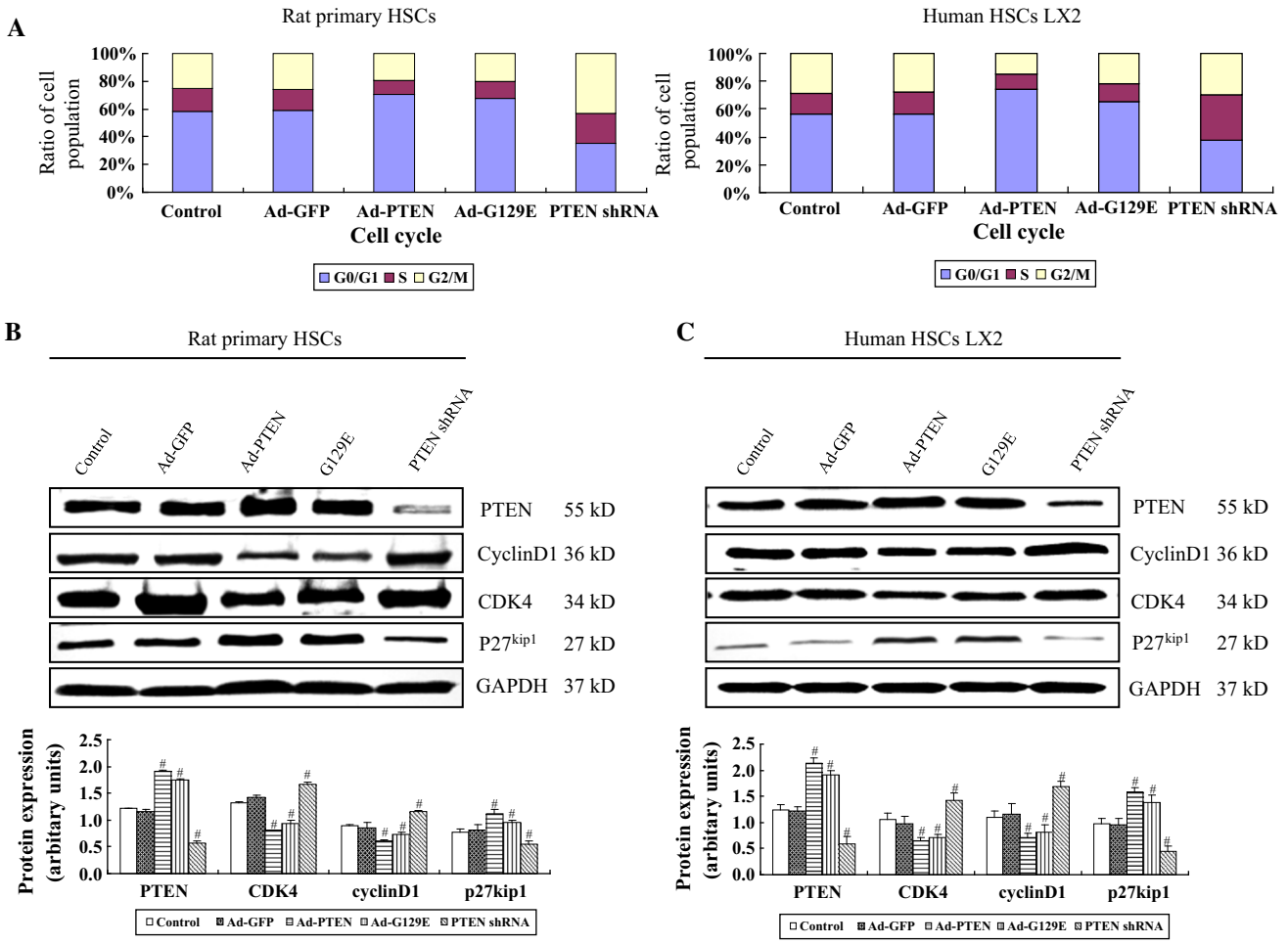

Fig. 2 The mechanism of recombinant adenovirus effects on cell cycles of HSCs at 72 h post-transfection. **a** Flow cytometry was used to check the cell cycles. At 72 h post-transfection, a significantly higher number of rat primary HSCs and human LX-2 cells was found in the G_0/G_1 phase in the Ad-PTEN (70.56 ± 4.05 vs 71.84 ± 2.15 %) and Ad-G129E groups (67.42 ± 2.15 vs 64.12 ± 1.25 %) than in the Ad-GFP group (58.78 ± 1.11 vs 56.37 ± 1.12 %), $P < 0.01$, and a significantly lower cell number was found in the PTEN shRNA group (35.46 ± 3.05 vs 37.98 ± 2.13 %) in comparison to the Ad-GFP group, $P < 0.01$. In the S phase, a significantly lower number of rat primary HSCs and human LX-2 cells was found in the Ad-PTEN (10.25 ± 1.04 vs 10.56 ± 1.15 %) and Ad-G129E groups (12.11 ± 1.05 vs 13.12 ± 3.12 %) in comparison to the Ad-GFP group (15.55 ± 1.74 vs 16.21 ± 2.13 %), $P < 0.01$, and significantly increased number of cells was observed in the PTEN shRNA group (21.17 ± 2.94 vs 33.34 ± 2.15 %) in comparison to the Ad-GFP group, $P < 0.01$. Cells in the G_2/M phase were also studied and found to be similar as cells in the S phase. **b**, **c** Western blot was used to check the cell cycle-associated protein expression for CyclinD1, CDK4 and $P27^{kip1}$. The results have shown that CyclinD1 (29.07 vs 15.12, 38.79 vs 19.31 %) and CDK4 (42.96 vs 34.51, 33.67 vs 27.55 %) protein expressions were significantly down-regulated in the Ad-PTEN and Ad-G129E groups in comparison to the Ad-GFP group ($P < 0.01$), while the $P27^{kip1}$ protein expression was significantly up-regulated (63.16 vs 38.10, 67.37 vs 45.26 %) in comparison to the Ad-GFP group ($P < 0.01$). The situation with PTEN shRNA was opposite

We then found that both p-FAK^{Tyr397} and p-ERK$_1$ protein expression in rat primary HSCs significantly decreased in the Ad-PTEN (0.42 ± 0.05 vs 0.25 ± 0.02) and Ad-G129E (0.49 ± 0.07 vs 0.28 ± 0.07) groups in comparison with the control (0.80 ± 0.09 vs 0.54 ± 0.07) and Ad-GFP (0.78 ± 0.05 vs 0.52 ± 0.06) groups ($P < 0.01$), while it significantly increased in the PTEN shRNA group (0.92 ± 0.07 vs 0.70 ± 0.05), $P < 0.01$ (Fig. 3a, b). A similar tendency was also found in experiments with human LX-2 cells (Fig. 3a, c). However, no significant differences were found in mRNA expressions of FAK and ERK (Fig. 3d, e). The data indicated that PTEN may regulate HSCs behavior via the FAK/ERK signaling pathway.

The Role of PTEN on CCl_4-Induced Rat Liver Fibrosis and the Activation of HSCs In Vivo

With the overexpressed PTEN gene in the Ad-PTEN and Ad-G129E groups, biochemical index analyses have shown that the over-expression of the PTEN gene in the Ad-PTEN

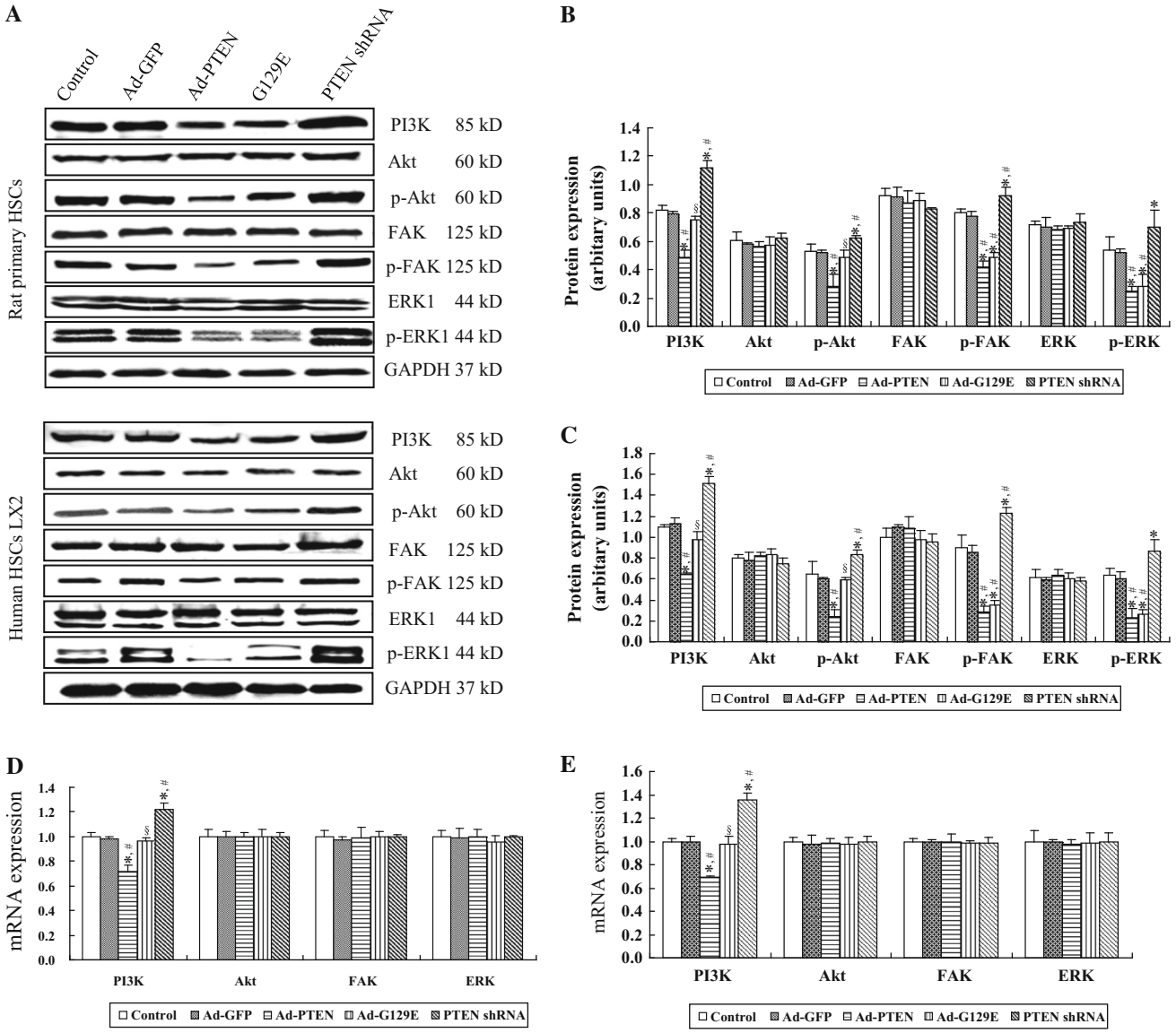

Fig. 3 The mechanisms of recombinant adenovirus on cell signaling transduction pathways in HSCs at 72 h post-transfection. **a**, **b** Western blot analysis has shown that, in rat primary HSCs, PI3K and p-Akt (Thr308), protein expression significantly decreased in the Ad-PTEN group (0.49 ± 0.02 vs 0.28 ± 0.02), in comparison with the Ad-G129E (0.75 ± 0.06 vs 0.48 ± 0.03), control (0.82 ± 0.07 vs 0.50 ± 0.02) and Ad-GFP groups (0.79 ± 0.03 vs 0.52 ± 0.05), $P < 0.01$, while it significantly increased in the PTEN shRNA group (1.12 ± 0.14 vs 0.62 ± 0.03) in comparison to the Ad-G129E and control groups ($P < 0.01$). Moreover, both p-FAK (Tyr397) and p-ERK$_1$ protein expression in rat primary HSCs significantly decreased in the Ad-PTEN (0.42 ± 0.05 vs 0.25 ± 0.02) and Ad-G129E groups (0.49 ± 0.07 vs 0.28 ± 0.07) in comparison with the control (0.80 ± 0.09 vs 0.54 ± 0.07) and Ad-GFP groups (0.78 ± 0.05 vs 0.52 ± 0.06), $P < 0.01$, while it significantly increased in the PTEN shRNA group (0.92 ± 0.07 vs 0.70 ± 0.05) in comparison with the Ad-G129E and control groups, $P < 0.01$. There were no significant differences between the Ad-G129E, control and Ad-GFP groups, $P > 0.05$. **c** A similar tendency was also found in experiments with human LX-2 cells. **d**, **e** Real time PCR was also used to check for mRNA changes in primary HSCs. Expression in the control group was arbitrarily assigned a value of 1; relative to this value, the PI3K mRNA expression levels in the Ad-GFP, Ad-PTEN, Ad-G129E and PTEN shRNA groups were 0.979-, 0.716-, 0.962- and 1.223-fold, respectively; however, no significant differences were found in mRNA expression levels of Akt, FAK and ERK. Similar results were observed in human LX-2 cells. $^{*}P < 0.01$, in comparison to the control group. $^{\#}P < 0.01$, compared to the Ad-GFP group $^{\S}P < 0.05$, compared to the Ad-PTEN group

and Ad-G129E groups could improve liver function by significantly reducing the serum levels of serum alanine aminotransferase (ALT) and aspartate aminotransferase (AST), in comparison to the CCl_4 group, control group and Ad-GFP group. However, the PTEN shRNA had the opposite effect (Table 3).

The hematoxylin and eosin (H&E) stain and the Masson's trichrome (MT) stain confirmed that the over-

Table 3 Impact of adenovirus-mediated PTEN gene therapy on AST and ALT in CCl_4-induced liver fibrosis at different time points (mean ± SD, $n = 3$)

Groups	ALT(U/L)	AST(U/L)
Tre 1 week		
Control	57.78 ± 8.23	146.78 ± 12.23
CCl_4	684.32 ± 78.34	840.32 ± 32.25
Ad-GFP	645.65 ± 34.26	832.12 ± 40.32
Ad-PTEN	384.98 ± 36.23[a]	398.43 ± 43.23[a]
Ad-G129E	495.34 ± 45.12[a]	546.32 ± 32.12[a]
PTEN shRNA	2030.31 ± 112.34[b]	1730.54 ± 87.34[b]
Tre 2 weeks		
Control	57.46 ± 3.58	142.34 ± 10.24
CCl_4	712.34 ± 34.54	843.23 ± 54.32
Ad-GFP	697.45 ± 45.76	876.34 ± 33.32
Ad-PTEN	338.12 ± 12.34[a]	407.34 ± 32.12[a]
Ad-G129E	364.32 ± 34.56[a]	408.67 ± 23.78[a]
PTEN shRNA	2040.21 ± 126.32[b]	1860.32 ± 210.32[b]
Tre 3 weeks		
Control	58.54 ± 6.58	148.45 ± 13.27
CCl_4	1892.32 ± 113.12	2018.32 ± 123.45
Ad-GFP	1746.32 ± 98.23	1879.23 ± 119.34
Ad-PTEN	524.35 ± 34.12[a]	690.35 ± 54.23[a]
Ad-G129E	576.23 ± 43.21[a]	820.43 ± 67.32[a]
PTEN shRNA	1937.56 ± 32.21[b]	2390.32 ± 112.23[b]
Tre 4 weeks		
Control	62.31 ± 8.12	155.37 ± 13.27
CCl_4	594.39 ± 32.18	1110.32 ± 89.34
Ad-GFP	576.45 ± 23.43	886.43 ± 45.67
Ad-PTEN	490.32 ± 32.23[a]	528.34 ± 32.12[a]
Ad-G129E	530.23 ± 22.56[a]	628.43 ± 45.34[a]
PTEN shRNA	1148.32 ± 54.32[b]	1270.34 ± 121.28[b]

[a] $P < 0.01$ versus CCl_4, Ad-GFP

[b] $P < 0.05$ versus CCl_4, Ad-GFP, Ad-PTEN

expressed PTEN gene in the Ad-PTEN and Ad-G129E groups reduced the hepatic cell necrosis, as well as liver inflammation (Fig. 4a, b) and also decreased collagen deposition in liver tissue (Fig. 4a, c). The mRNA of collagen α1 (I) was further checked by real-time PCR and has shown a similar tendency (Fig. 4d). To explore whether improved pathology was due to the changes in PTEN expression, we performed immunofluorescent staining for PTEN in green and α-SMA in red; the yellow color from the co-localization showed that the $PTEN^{+}$HSCs, which mainly existed in the cytoplasm of activated HSCs, and the activated HSCs expressing PTEN, accounted for a decreasing percentage of total activated HSCs. This observation indicated that the over-expression of PTEN induced by exogenous wild-type PTEN and G129E genes can significantly inhibit the α-SMA expression in comparison with the Ad-GFP and CCl_4 groups (Fig. 4). We found that PTEN expression significantly decreased with administration of the Ad-PTEN and Ad-G129E recombinant adenovirus, which confirmed successful infection and was evident through improved pathology (Fig. 4a).

We isolated the total protein from liver tissues in each group and performed Western blot analysis to further check the protein expressions of PTEN and α-SMA. Consistent with our previous studies, the PTEN protein expression decreased significantly due to CCl_4 whereas α-SMA protein expression increased significantly due to CCl_4 [18]. The PTEN protein expression increased significantly by 1.96-, 3.20-, 3.33- and 5.64-fold in the Tre 1 week, Tre 2 weeks, Tre 3 weeks and Tre 4 weeks ($P < 0.01$) in rats treated by Ad-PTEN (Fig. 5a). The α-SMA protein changes had an opposite effect in comparison to PTEN (Fig. 5b).

The Role of PTEN on CCl_4-Induced Rat Liver Fibrosis and the Apoptosis of HSCs In Vivo

In our previous study, TUNEL was used to find that CCl_4 treatment can increase the levels of apoptotically activated HSCs in comparison to normal rat liver tissue, where less apoptotically activated HSCs were detected [18]. In this experiment, the over-expression of the PTEN gene induced by exogenous wild-type PTEN and G129E genes can induce the apoptosis of activated HSCs. The ratio of apoptotically activated HSCs to total activated HSCs was described as the apoptotic index. We found a significantly increased apoptotic index in the Ad-PTEN group in Tre 1 week (65.12 ± 5.37 %), Tre 2 weeks (46.32 ± 4.26 %), Tre 3 weeks (30.16 ± 2.23 %) and Tre 4 weeks (32.14 ± 1.35 %) groups, in comparison to CCl_4 and Ad-GFP groups ($P < 0.01$); the PTEN shRNA induced down-regulation of PTEN can caused significantly reduced apoptotic index of HSCs, $P < 0.05$ (Table 4).

Discussion

Liver fibrosis is reversible, however, there is no effective therapy to reverse hepatic fibrosis and stop the progression to irreversible cirrhosis [1, 2]. An increased number of myofibroblasts was found to be associated with the severity of liver fibrosis in patients [3].

PTEN is involved in the pathogenesis of myocardial, renal and lung fibrosis [14, 15, 24]. Our previous studies have found that increased PTEN expression can reduce the number of activated HSCs, negatively regulate fibrogenesis in vivo [17, 18], and induce the apoptosis of activated HSCs in vitro [20]. The activation and apoptosis of HSCs

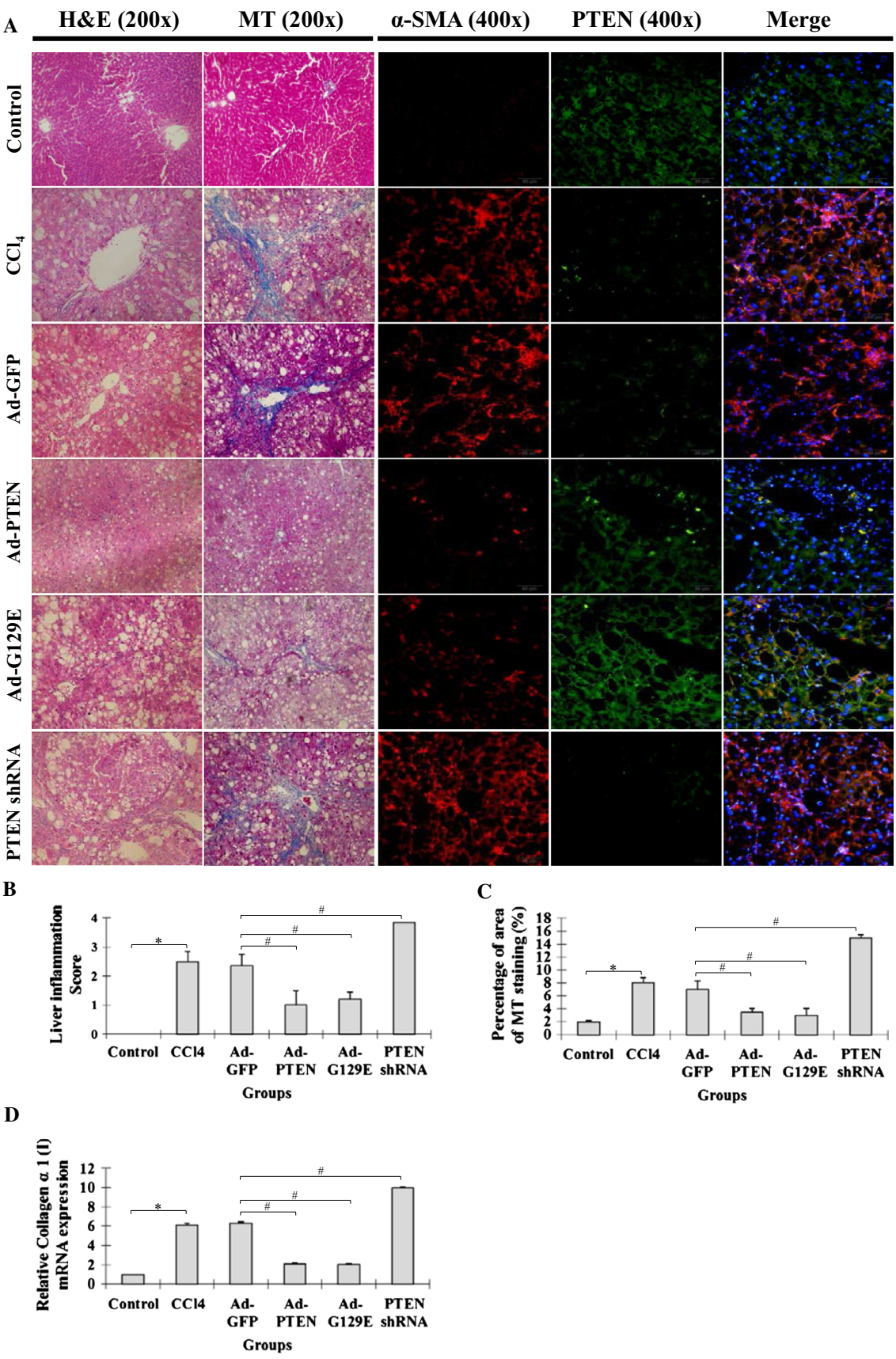
A
H&E (200x)
MT (200x)
α-SMA (400x)
PTEN (400x)
Merge
Control
CCl4
Ad-GFP
Ad-PTEN
Ad-G129E
PTEN shRNA
B
Liver inflammation Score
Control
CCl4
Ad-GFP
Ad-PTEN
Ad-G129E
PTEN shRNA
Groups
C
Percentage of area of MT staining (%)
Control
CCl4
Ad-GFP
Ad-PTEN
Ad-G129E
PTEN shRNA
Groups
D
Relative Collagen α 1 (I) mRNA expression
Control
CCl4
Ad-GFP
Ad-PTEN
Ad-G129E
PTEN shRNA
Groups

◀**Fig. 4** Over-expression of PTEN ameliorated the CCl_4-induced rat hepatic fibrosis and decreased activated HSCs in the liver tissues, whereas down-regulation of PTEN by shRNA aggravated hepatic fibrosis and increased activated HSCs in vivo. **a**, **b** The hematoxylin and eosin (H&E) stain (×200) and (**a**, **c**) the Masson's trichrome (MT) stain (×200) showed less necrosis of hepatic cells and collagen deposition in the liver tissue by an over-expressed PTEN gene in the Ad-PTEN and Ad-G129E groups, as well as the mRNA changes of collagen α1 (I) (**d**). **a** Immunofluorescent staining was also used for PTEN in *green* and α-SMA in *red*. The *yellow color* from co-localization showed the $PTEN^{+}$HSCs mainly existed in the cytoplasm of activated HSCs. Activated HSCs expressing PTEN accounted for a decreasing percentage of the total activated HSCs, which indicated that the over-expression of PTEN induced by the exogenous wild-type PTEN gene and G129E gene can significantly inhibit the α-SMA expression compared with the Ad-GFP and CCl_4 grous. PTEN expression was significantly increased with the Ad-PTEN and Ad-G129E recombinant adenovirus in the treatment group, which confirmed successful infection, which was manifested through improved pathology. $^{*}P < 0.01$, compared to the control group. $^{\#}P < 0.01$, compared to the Ad-GFP group

plays a key role in liver fibrogenesis [2], which shows that PTEN is a potential target for reversing liver fibrosis.

To address this question, we first isolated and purified rat primary HSCs and then performed transfection using the PTEN over-expressing recombinant adenovirus Ad-PTEN and Ad-G129E. In addition, transfection was performed with the PTEN under-expressing recombinant adenovirus PTEN shRNA and a secondary cell line, Human LX-2, was used. We found that PTEN expression was up-regulated by Ad-PTEN and Ad-G129E and down-regulated by PTEN shRNA. Increased PTEN expression led to decreased activation of HSCs and increased apoptosis of both rat primary HSCs and human LX-2 cells, which was consistent with previous findings [18, 20, 25]. This study additionally found that down-regulated PTEN expression resulted in more pronounced liver fibrosis in vivo, increased activated HSCs and decreased apoptotically activated HSCs, which indicated a protective role of PTEN in hepatic fibrosis.

The proliferation and migration of HSCs in the liver play a critical role in fibrostenosis [1]. Increased PTEN expression led to a reduction in the proliferation of HSCs in vitro, and also improved the fibrotic phenotype in CCl_4-treated rats, while a decreased expression of PTEN acted oppositely. Activated HSCs rarely can return to a quiescent condition; however, the induction of apoptosis of activated HSCs is one of the major ways for liver to eliminate activated HSCs [26]. In this study, increased PTEN expression caused an increase in apoptotic HSCs, and decreased PTEN expression resulted in decreased apoptotic HSCs in both rat primary HSCs and human LX-2 cells, pointing to a pro-apoptotic role of PTEN in HSCs. The activation of caspase-3, sharing lots of typical characteristics with the other caspase, is one of the signaling pathways in HSCs apoptosis [27, 28]. To further investigate the

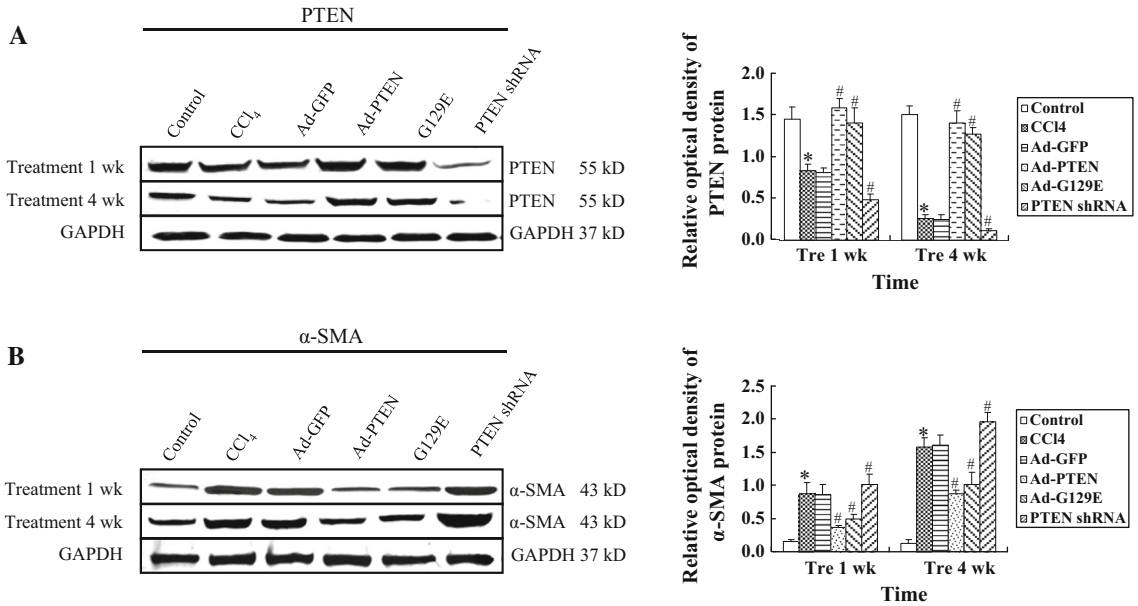

Fig. 5 PTEN and α-SMA protein expressions were changed by transfection in vivo. **a** Western blot results showed that PTEN protein expression in rats treated by Ad-PTEN increased by 1.96-, 3.20-, 3.33- and 5.64-fold in the treatment (Tre) 1 week, Tre 2 weeks, Tre 3 weeks and Tre 4 weeks in comparison to the CCl_4 groups ($P < 0.01$). **b** α-SMA protein expression determined by Western blot was significantly decreased by Ad-PTEN to 56.98, 60.53, 63.86 and 63.35 % in Tre 1 week, Tre 2 weeks, Tre 3 weeks and Tre 4 weeks, in comparison to the Ad-GFP group ($P < 0.01$), respectively. $^{*}P < 0.01$, compared to control group. $^{\#}P < 0.01$, compared to Ad-GFP group

Table 4 Effects of PTEN on HSCs apoptosis in rat liver fibrosis, induced by CCl_4 by TUNEL (mean ± SD, $n = 3$)

Groups	Apoptotic rates (%)				
	CCl_4	Ad-GFP	Ad-PTEN	Ad-G129E	PTEN shRNA
Tre 1 week	3.95 ± 0.03	6.11 ± 0.05	65.12 ± 5.37[a]	35.24 ± 0.11	0.65 ± 0.03[b]
Tre 2 weeks	2.76 ± 0.05	5.23 ± 0.16	46.32 ± 4.26[a]	25.37 ± 2.35[a]	0.43 ± 0.01[b]
Tre 3 weeks	1.21 ± 0.01	3.21 ± 0.05	30.16 ± 2.23[a]	17.21 ± 1.56[b]	0.39 ± 0.02[b]
Tre 4 weeks	0.75 ± 0.03	2.56 ± 0.23	32.14 ± 1.35[a]	20.25 ± 2.17[b]	0.24 ± 0.06[b]

The apoptotic index increased in the Ad-PTEN and Ad-G129E groups in comparison to the CCl_4 and Ad-GFP groups; the PTEN shRNA caused a significantly reduced apoptotic index in HSCs in comparison to the CCl_4 and Ad-GFP group

[a] $P < 0.01$, compared to the CCl_4 group, Ad-GFP group

[b] $P < 0.05$, compared to the CCl_4, Ad-GFP, and Ad-PTEN groups

potential mechanism of PTEN in HSCs apoptosis, caspase-3 activity was assessed. We found that increased PTEN expression led to enhanced caspase-3 activity, which was consistent with an increased apoptotic index in both rat primary HSCs and human LX-2 cells treated by Ad-PTEN and Ad-G129E. The PTEN shRNA reduced PTEN expression and down-regulated the activity of caspase-3, which was also consistent with the results that a decreased expression of the PTEN gene resulted in less apoptotic HSCs. Overall, our data have shown that PTEN can induce HSCs apoptosis, probably by regulating caspase-3 activity.

The balance of apoptosis-associated genes Bcl-2 and Bax plays an important role in cell apoptosis [29]. We found that the anti-apoptosis factor Bcl-2 increased in HSCs treated by PTEN shRNA and decreased in HSCs treated by Ad-PTEN and Ad-G129E, while its inhibitor Bax was decreased in PTEN shRNA treated HSCs and increased in Ad-PTEN and Ad-G129E treated HSCs. It was concluded that PTEN may regulate HSCs apoptosis through Bax/Bcl-2 expression.

Earlier studies have found that PTEN negatively regulates the cell cycle and inhibits the proliferation and differentiation of tumor cells [30, 31]. The question remained whether PTEN can regulate the cell cycle of HSCs based on the inhibition of activation and proliferation of HSCs from over-expressed PTEN [20]. The results have shown that high PTEN expression can arrest the HSCs cell cycle in the G_0/G_1 phase probably due to inhibition of the G_1/S phase transformation. Moreover, the low expression of PTEN can promote the transformation of the G_1/S phase. CyclinD1, a positive regulatory factor on the G_1/S phase transformation, as well as CDK4, a major regulator in the cell cycle, were found to increase with down-regulation of PTEN expression. This could partially explain the mechanism of PTEN on the arrest of G_0/G_1 in HSCs. This finding was consistent with the negative regulatory role of PTEN on the cell cycle of tumor cells, through inhibition of CyclinD1 and CDK4 protein expressions [32, 33]. $P27^{kip1}$ binds specifically to CyclinD-CDK4(CDK6), CyclinA-CDK2 and CyclinE2-CDK2, which all have an important role in the S phase. The lower level of $P27^{kip1}$ cannot efficiently inhibit the cell over-proliferation and tumor progression [34]. In this study, the over-expressed PTEN gene has been shown to enhance $P27^{kip1}$ expression, indicating that PTEN may negatively regulate the HSCs cell cycle through $P27^{kip1}$.

The behavior of HSCs is regulated by several signal transduction pathways, such as focal adhesion kinase (FAK)/extracellular signal-regulated kinase1/2 (ERK1/2), phosphoinositol-3-kinase (PI3K)/serine–threonine protein kinase B (Akt), Ras/Raf/MEK/ERK1/2, etc. [21, 35, 36]. The PTEN was found to be involved in signaling pathways in HSCs and other types of cells [9, 10, 37–40], indicating a potential relationship between the PTEN and behavior regulation of HSCs.

The reduced expression of PTEN in this study was found to promote p-Akt^{Thr308} expression through lipid phosphatase activity in the HSCs and positively regulate PI3K/Akt signaling, leading to increased activation and decreased apoptosis of HSCs. The over-expression of PTEN can inhibit PI3K/Akt signaling. FAK, the key point in the integrin-mediated signal transduction pathway, was recently found to play a vital role in the development of fibrotic disorders [41]. We have previously shown that the decrease in FAK expression using FAK shRNA inhibited proliferation and induced the apoptosis of the rat HSCs cell line [21]. In this study, we used PTEN shRNA to achieve the reduced expression of PTEN in rat primary HSCs and human LX-2 cells, and we found increased p-FAK^{Tyr397} and p-ERK expressions. In addition, we also detected that the over-expressed PTEN can negatively regulate the FAK/ERK signaling pathway in HSCs through the protein phosphatase activity, leading to decreased HSCs activation.

Gene therapy using the adenovirus vector is a potentially novel method of transfection efficiency with a low number of adverse effects [42–44]. In this study, the treatment of rats with CCl_4-induced hepatic fibrosis with a recombinant adenovirus carrying the highly expressed PTEN gene has

been shown to improve liver function, inhibit activated HSCs and induce apoptosis of active HSCs. The down-regulated PTEN can worsen hepatic fibrosis in the CCl_4-induced rat model.

In conclusion, these data demonstrate that PTEN can regulate HSCs' behavior both in vitro and in vivo, probably through the FAK/ERK and PI3K/Akt signaling pathways and also through its regulation on the HSCs cell cycle and caspase-3 activity. Gene therapy using recombinant adenovirus encoding the wild-type PTEN may be a novel treatment option for hepatic fibrosis.

Acknowledgments This work was supported by the National Natural Science Foundation of China (Grant 30872513), Natural Science Foundation of Hebei Province (Grant C2010000565), and Hebei Provincial Science and Technology Department (Grant 09966108D). The authors would like to thank the foundations for their support. We appreciate Gregory X Shen for his valuable revision of written English and owe many thanks to Hong Zhang and Jinbo Guo for their photo contributions.

Compliance with ethical standards

Conflict of interest The authors have declared no conflict of interest.

References

1. Hernandez-Gea V, Friedman SL. Pathogenesis of liver fibrosis. *Annu Rev Pathol*. 2011;6:425–456.
2. Friedman SL. Mechanisms of hepatic fibrogenesis. *Gastroenterology*. 2008;134:1655–1669.
3. Brenner DA, Kisseleva T, Scholten D, et al. Origin of myofibroblasts in liver fibrosis. *Fibrogenesis Tissue Repair*. 2012; 5:S17.
4. Asahina K, Zhou B, Pu WT, Tsukamoto H. Septum transversum-derived mesothelium gives rise to hepatic stellate cells and perivascular mesenchymal cells in developing mouse liver. *Hepatology*. 2011;53:983–995.
5. Scholten D, Reichart D, Paik YH, et al. Migration of fibrocytes in fibrogenic liver injury. *Am J Pathol*. 2011;179:189–198.
6. Wasmuth HE, Weiskirchen R. Pathogenesis of liver fibrosis: modulation of stellate cells by chemokines. *Z Gastroenterol*. 2010;48:38–45.
7. Kisseleva T, Cong M, Paik Y, et al. Myofibroblasts revert to an inactive phenotype during regression of liver fibrosis. *Proc Natl Acad Sci USA*. 2012;109:9448–9453.
8. Liu X, Xu J, Brenner DA, Kisseleva T. Reversibility of liver fibrosis and inactivation of fibrogenic myofibroblasts. *Curr Pathobiol Rep*. 2013;1:209–214.
9. Kim HA, Kim KJ, Seo KH, Lee HK, Im SY. PTEN/MAPK pathways play a key role in platelet-activating factor-induced experimental pulmonary tumor metastasis. *FEBS Lett*. 2012; 586:4296–4302.
10. Shi Y, Paluch BE, Wang X, Jiang X. PTEN at a glance. *J Cell Sci*. 2012;125:4687–4692.
11. Garcia-Junco-Clemente P, Golshani P. PTEN: a master regulator of neuronal structure, function, and plasticity. *Commun Integr Biol*. 2014;7:e28358.
12. Muniyan S, Ingersoll MA, Batra SK, Lin MF. Cellular prostatic acid phosphatase, a PTEN-functional homologue in prostate epithelia, functions as a prostate-specific tumor suppressor. *Biochim Biophys Acta*. 2014;1846:88–98.
13. White ES, Thannickal VJ, Carskadon SL, et al. Integrin α4β1 regulates migration across basement membranes by lung fibroblasts: a role for phosphatase and tensin homologue deleted on chromosome 10. *Am J Respir Crit Care Med*. 2003;168:436–442.
14. White ES, Atrasz RG, Hu B, et al. Negative regulation of myofibroblast differentiation by PTEN (phosphatase and tensin homolog deleted on chromosome 10). *Am J Respir Crit Care Med*. 2006;173:112–121.
15. Lan R, Geng H, Polichnowski AJ, et al. PTEN loss defines a TGF-β-induced tubule phenotype of failed differentiation and JNK signaling during renal fibrosis. *Am J Physiol Renal Physiol*. 2012;302:F1210–F1223.
16. Vinciguerra M, Veyrat-Durebex C, Moukil MA, Rubbia-Brandt L, Rohner-Jeanrenaud F, Foti M. PTEN down-regulation by unsaturated fatty acids triggers hepatic steatosis via an NF-κBp65/mTOR-dependent mechanism. *Gastroenterology*. 2008; 134:268–280.
17. Hao LS, Zhang XL, An JY, et al. PTEN expression is down-regulated in liver tissues of rats with hepatic fibrosis induced by biliary stenosis. *APMIS*. 2009;117:681–691.
18. Zheng L, Chen X, Guo J, et al. Differential expression of PTEN in hepatic tissue and hepatic stellate cells during rat liver fibrosis and its reversal. *Int J Mol Med*. 2012;30:1424–1430.
19. Ma J, Li F, Liu L, et al. Raf kinase inhibitor protein inhibits cell proliferation but promotes cell migration in rat hepatic stellate cells. *Liver Int*. 2009;29:567–574.
20. Hao LS, Zhang XL, An JY, et al. Adenoviral transduction of PTEN induces apoptosis of cultured hepatic stellate cells. *Chin Med J (Engl)*. 2009;122:2907–2911.
21. An J, Zheng L, Xie S, et al. Down-regulation of focal adhesion kinase by short hairpin RNA increased apoptosis of rat hepatic stellate cells. *APMIS*. 2011;119:319–329.
22. Knodell RG, Ishak KG, Black WC, et al. Formulation and application of a numerical scoring system for assessing histological activity in asymptomatic chronic hepatitis. *Hepatology*. 1981;1:431–435.
23. Wang Y, Gao J, Zhang D, et al. New insights into the antifibrotic effects of sorafenib on hepatic stellate cells and liver fibrosis. *J Hepatol*. 2010;53:132–144.
24. Singla DK. Akt-mTOR pathway inhibits apoptosis and fibrosis in doxorubicin-induced cardiotoxicity following embryonic stem cell transplantation. *Cell Transplant*. 2015;24:1031–1042.
25. Takashima M, Parsons CJ, Ikejima K, Watanabe S, White ES, Rippe RA. The tumor suppressor protein PTEN inhibits rat hepatic stellate cell activation. *J Gastroenterol*. 2009;44:847–855.
26. Povero D, Busletta C, Novo E, et al. Liver fibrosis: a dynamic and potentially reversible process. *Histol Histopathol*. 2010;25: 1075–1091.
27. Che XH, Jiang WY, Parajuli DR, Zhao YZ, Lee SH, Sohn DH. Apoptotic effect of propyl gallate in activated rat hepatic stellate cells. *Arch Pharm Res*. 2012;35:2205–2210.
28. Li J, Li X, Xu W, et al. Antifibrotic effects of luteolin on hepatic stellate cells and liver fibrosis by targeting AKT/mTOR/p70S6 K and TGFβ/Smad signalling pathways. *Liver Int*. 2015;35: 1222–1233.
29. Marin JJ, Hernandez A, Revuelta IE, et al. Mitochondrial genome depletion in human liver cells abolishes bile acid-induced apoptosis: role of the Akt/mTOR survival pathway and Bcl-2 family proteins. *Free Radic Biol Med*. 2013;61:218–228.
30. Van Duijn PW, Ziel-van der Made AC, van der Korput JA, Trapman J. PTEN-mediated G1 cell-cycle arrest in LNCaP prostate cancer cells is associated with altered expression of cell-cycle regulators. *Prostate*. 2010;70:135–146.

31. Paul-Samojedny M, Suchanek R, Borkowska P, et al. Knockdown of AKT3 (PKBγ) and PI3KCA suppresses cell viability and proliferation and induces the apoptosis of glioblastoma multiforme T98G cells. *Biomed Res Int*. 2014;2014:768181.
32. Aarts M, Linardopoulos S, Turner NC. Tumour selective targeting of cell cycle kinases for cancer treatment. *Curr Opin Pharmacol*. 2013;13:1–7.
33. Chung JH, Ostrowski MC, Romigh T, Minaguchi T, Waite KA, Eng C. The ERK1/2 pathway modulates nuclear PTEN-mediated cell cycle arrest by cyclin D1 transcriptional regulation. *Hum Mol Genet*. 2006;15:2553–2559.
34. Mitrea DM, Yoon MK, Ou L, Kriwacki RW. Disorder-function relationships for the cell cycle regulatory proteins p21 and p27. *Biol Chem*. 2012;393:259–274.
35. Brenner DA. Molecular pathogenesis of liver fibrosis. *Trans Am Clin Climatol Assoc*. 2009;120:361–368.
36. Wang J, Xu F, Zhu D, et al. Schistosoma japonicum soluble egg antigens facilitate hepatic stellate cell apoptosis by downregulating Akt expression and upregulating p53 and DR5 Expression. *PLoS Negl Trop Dis*. 2014;8:e3106.
37. Zhang S, Yu D. PI(3)king apart PTEN's role in cancer. *Clin Cancer Res*. 2010;16:4325–4330.
38. Ming M, Han W, Maddox J, et al. UVB-induced ERK/AKT-dependent PTEN suppression promotes survival of epidermal keratinocytes. *Oncogene*. 2010;29:492–502.
39. Bunney TD, Katan M. Phosphoinositide signalling in cancer: beyond PI3K and PTEN. *Nat Rev Cancer*. 2010;10:342–352.
40. Dubrovska A, Kim S, Salamone RJ, et al. The role of PTEN/Akt/PI3K signaling in the maintenance and viability of prostate cancer stem-like cell populations. *Proc Natl Acad Sci USA*. 2009;106:268–273.
41. Lagares D, Kapoor M. Targeting focal adhesion kinase in fibrotic diseases. *BioDrugs*. 2013;27:15–23.
42. Podolska K, Stachurska A, Hajdukiewicz K, Malecki M. Gene therapy prospects-intranasal delivery of therapeutic genes. *Adv Clin Exp Med*. 2012;21:525–534.
43. Sakashita M, Mochizuki S, Sakurai K. Hepatocyte-targeting gene delivery using a lipoplex composed of galactose-modified aromatic lipid synthesized with click chemistry. *Bioorg Med Chem*. 2014;22:5212–5219.
44. Baertsch MA, Leber MF, Bossow S, et al. MicroRNA-mediated multi-tissue detargeting of oncolytic measles virus. *Cancer Gene Ther*. 2014;21:373–380.